



ISSN: 0067-2904

## Building 1D Mechanical Earth Model for Subba Oilfield in Iraq

Mohammed Al-Jawad, Worood Al-Zubaidy\*

Department of Petroleum Engineering, College of Engineering, University of Baghdad, Baghdad, Iraq

Received: 2/1/2023

Accepted: 18/3/2023

Published: 29/2/2024

### Abstract

At the Subba oil field, wellbore stability is the main concern while drilling. The wellbore's instability causes several issues, including: (inefficient hole cleaning, tight hole, stuck pipe, mud losses, caving, bad cementing, and well kick or blowout). This increases Non-Productive Time (NPT) and well-drilling costs; hence the operator's main goal is to create a drilling program that reduces these problems and therefore reduce drilling cost. The study aims to build a 1D mechanical earth model to predict the wellbore failure and design optimum mud weight to improve the drilling efficiency for future wells. The model includes pore pressure, stress state, and rock mechanical parameters (such as UCS, angle of friction, Young-Modulus, and Poisson-Ratio). To achieve this aim, the study utilised offset well data including log data (Gamma-Ray Logs (GR), Caliper Logs (CALI), Density Logs (RHOZ), and Compressional Sonic (DTCO) and Shear Sonic (DTSM)), Core tests, Mini-frac field tests, Drilling Reports, Mud Reports, and Mud Log Reports (master log) to estimate and calibrate the profiles of formation pore pressure, rock mechanical properties, and in-situ stresses.

The 1D mechanical earth model was built using the Excel program for three wells data set, where all the necessary parameters to create the model was calculated, calibrated for the calculated variables with core data and pressure test points, and finally the safe mud window was detected.

The results showed that the Eaton Slowness method to predict pore pressure perfectly matches the pressure test points. The most common fault regimes in the Subba oilfield are normal and strike-slip faults. The Modified Lade criteria showed a compatible match with drilling events and calliper log in predicting the failure zones, so it is the best criterion in determining minimum and maximum mud weight. Based on the results of this study and in comparison with the mud window used in drilling operations in the field, it is necessary to change the mud window used in drilling and adopt the safe MWW of this study in drilling new wells in this field and the area adjacent to the field.

**Keywords:** Subba Oilfield, Hole problem, Wellbore Failure, NPT.

### بناء نموذج جيوميكانيكي احادي البعد لحقل صبة النفط في العراق

محمد الجواد, ورود عبد العباس\*

قسم هندسة النفط, كلية الهندسة, جامعة بغداد, بغداد, العراق

\*Email: [engineerworood1989@gmail.com](mailto:engineerworood1989@gmail.com)

## الخلاصة

يعتبر استقرار جدار البئر في حقل صبة هو العامل الرئيسي اثناء عمليات الحفر. عدم استقرار جدار البئر يسبب العديد من المشاكل منها: انهيار جدار البئر، التكوينات الرخوة، استعصاء الانابيب، فقدان دورة سائل الحفر، التكهف، رداءة السمنت، الرقصة او الانفجار). وهذا يؤدي الى زيادة الوقت وكذلك زيادة كلفة الحفر، وبالتالي فأن الهدف الرئيسي للمشغل هو اعداد برنامج حفر يقلل من تلك المشاكل وبالنتيجة تقل كلفة الحفر. تهدف الدراسة الى بناء نموذج جيوميكانيكي احادي البعد للتنبؤ بفشل جدار البئر وتصميم نافذة طين مثلى لتحسين كفاءة الحفر للأبار المستقبلية، الموديل يتضمن: الضغط المسامي، الاجهادات، الخواص الميكانيكية للصخور (مثل قوة الانضغاط غير المحصورة، زاوية الاحتكاك، معمل يونك، نسبة بويسون). لتحقيق ذلك الهدف، تتطلب الدراسة بيانات كاملة للأبار تتضمن بيانات تخطيط البئر ( Gama-Ray, Caliper Logs, Density Logs, Compressional Sonic and Shear Sonic), فحوصات اللباب، فحوصات الضغوط، تقارير الحفر وتقارير سائل الحفر لحساب ومعايرة الضغط الطبقي وخواص الصخور والاجهادات. تم بناء النموذج الجيوميكانيكي احادي البعد باستخدام برنامج الاكسل ولثلاثة آبار، حيث تم حساب جميع المعاملات الضرورية لإنشاء الموديل، بعدها تمت معايرة المتغيرات المحسوبة مع فحوصات اللباب وفحوصات الضغوط، وبانتهاء تم تحديد نافذة الطين الآمنة. اظهرت النتائج ان طريقة (Eaton Slowness) للتنبؤ بالضغط المسامي تعطي تطابق جيد مع فحوصات الضغط، وان انظمة الصدع الشائعة في حقل صبة هي (normal and strike slip)، وان قوة الانضغاط المحصورة وزاوية الاحتكاك الداخلي هما من اكثر معاملات الصخور تأثيرا على معيار الفشل، وان معيار الفشل (Modified Lade) اعطى تطابق متوافق مع احداث الحفر و ال (caliper log) من حيث التنبؤ بمناطق الفشل في جدار البئر، لذا فهو المعيار الافضل في التنبؤ بالحد الاعلى والأدنى لوزن الطين. بالاعتماد على نتائج هذه الدراسة وبمقارنتها مع نافذة الطين المستخدمة بعمليات الحفر في الحقل، فإنه من الضروري تغيير نافذة الطين المستخدمة في الحفر واعتماد نتائج هذه الدراسة من حيث استخدام النافذة الآمنة التي توصي بها الدراسة لحفر آبار جديدة في الحقل وفي المناطق المجاورة للحقل.

## 1. Introduction

In the petroleum and gas industry, the term "wellbore stability" is used to define the useable condition of the borehole while drilling operations are taking place. For a hole to be considered useable, it must be capable of accommodating logging, open-hole evaluations, casing runs, and other drilling activities satisfactorily. Hole collapse, tight holes, stuck pipes, insufficient hole cleaning, hole enlargement, flow, fracture, and lost circulation are some of the issues that must be addressed. Most borehole issues resulting in increased drilling expenses are linked to unstable wellbore conditions [1, 2]. These issues are primarily brought about by the imbalance that is generated between the rock strengths and the induced stresses once wellbore drilling has been completed. In-situ stress system plays the most crucial role in wellbore stability. When a well is drilled, the rock surrounding the hole must support the weight of the rock removed. Because of this, the in-situ tensions close to the borehole wall have been dramatically altered. This is demonstrated by the formation of a higher level of tension around the hole's wall, also known as a stress concentration. Depending on the rock's strength in that area, the stress concentration could cause the rock that makes up the borehole wall to break. For a borehole not to fail, drilling engineers must handle the stress concentration correctly. This can be achieved by altering the internal wellbore pressure and the borehole's direction concerning the forces in the surrounding environment. In most cases, the orientation of the borehole cannot be changed very much from its original state. Wellbore instability can be avoided by controlling the density of drilling mud pumped into the well. No matter how strong the rock is or how stressed the field is, the primary objective of the drilling mud pressure is to stop the pore fluid from flowing into the well. This is the case regardless of the field stresses. Due to the in situ stresses, which are greater than the pore pressure, the mud pressure generally necessary to hold the borehole wall

is greater than that required to balance and contain fluids [3]. Failure of the wall is caused by a brittle rock, resulting in the growth or collapse of the hole. Poor cementing, issues interpreting logs and responding to them, and poor directional controlling are signs of this condition. Inadequate cementing of the casing may result in difficulties with perforating, maintaining sand control, producing fluids, and stimulating the well. In addition, once the hole begins to collapse, small fragments of the formations may fall to the ground and block off the annulus. (Also known as hole pack-off), whereas medium to large fragments fall into the holes and may cause the drill string to become stuck. This occurs when the hole begins to collapse (i.e., hole bridging). They may make the string could not be pulled out. (i.e., a stuck pipe), and as a result, the activities that were planned have been put on hold. A stuck pipe problem due to hole collapse [3] is illustrated in Figure 1. So the prediction of the maximum and minimum mud weight are the primary objective of this study, and therefore reduce NPT (around 54% of the drilling time for the well SU\_20 was attributable to the NPT, according to an analysis of the breakdown time shown in Figure 2, what distinguishes this paper is the use of ten different formations in Subba oil field: Tanuma, Khasib, Mishrif, Rumaila, Ahmady, Maudud, Nahr Umr, Shuaiba and Zubair were investigated. There are two variables for the 1D MEM for construction: rock mechanical properties and stress data. Young modulus, poisson ratio, internal friction angle, cohesion, tensile strength and uniaxial compressive strength are the rock mechanical parameters. Overburden stress, horizontal stresses and pore pressure are the effective stress variables.

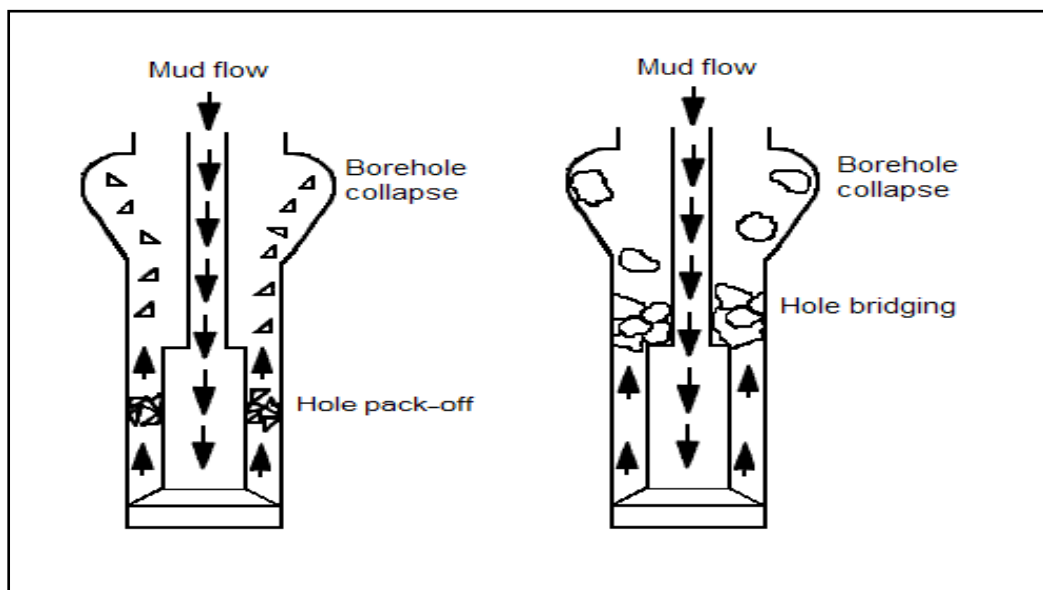


**Figure 1:** stuck pipe.

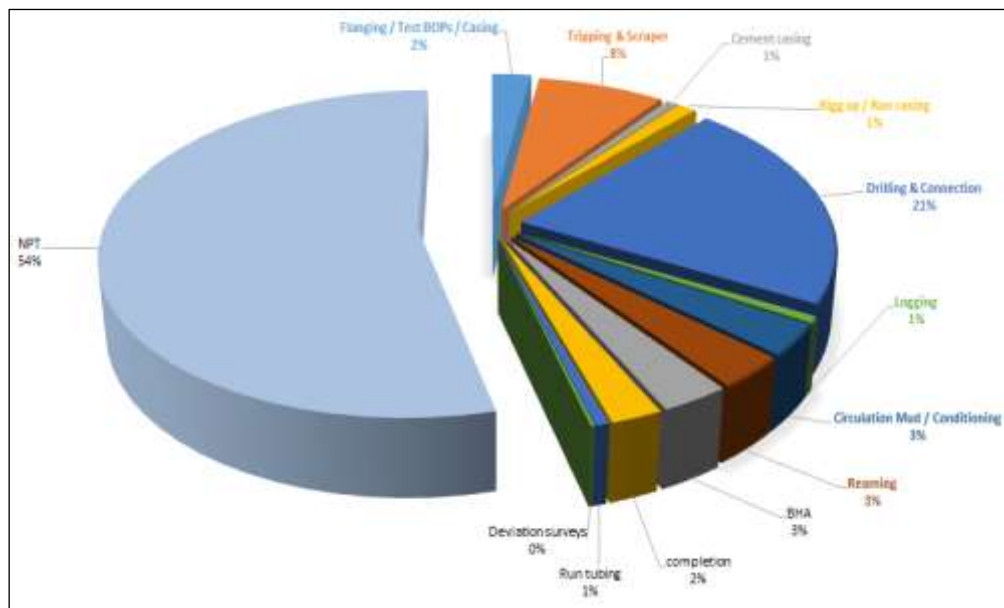


**Figure 2 :** Time breakdown for well SU\_20

## 2. Case of Study

The oil field of Subba is located in southern Iraq (Figure 3), in Thi Qar governorate, approximately (70 km) southeast of Nasiriya city, (110 km) northwest of Basra, and (12 km) northwest of the Luhais oil field [4]. It was discovered in 1954 and produced for the first time in 1990. The field's length is 30 km, while its width is 7 km. This field is situated on the Arabian platform's unstable shelf in the Zubair subzone at the western edge of the Mesopotamian Basin [5]. The southern and northern domes of the Subba oil field are separated by the shallow saddle, creating an asymmetrical anticlinal structure [6]. The little dome is situated in the north, whereas the large dome is situated in the south. The geological column for the Subba oilfield is presented in Figure 4. Hydrocarbon production in the Subba oilfield is predominantly from Nahr Umr, Zubair, and Yamamma formations [7], [8]. Subba oil field wells typically include four-part structures; 26", 17.5", 12.25 "and 8.375". Sections 12.25" and 8.375" are among those that provide the most significant difficulties and risks for the drilling activities in the Subba oil field. Significant challenges in drilling these sections include lost circulation issues in the Hartha formation and wellbore stability concerns in the Tanuma, Nahr Umr, and Zubair formations. Insufficient hole cleaning, a tight hole, a stuck pipe, a loss of circulation, poor cementing, and a well kick or blowout are all examples of problems that contribute to well instability. Hence, the drilling costs and NPT of the well both rises.

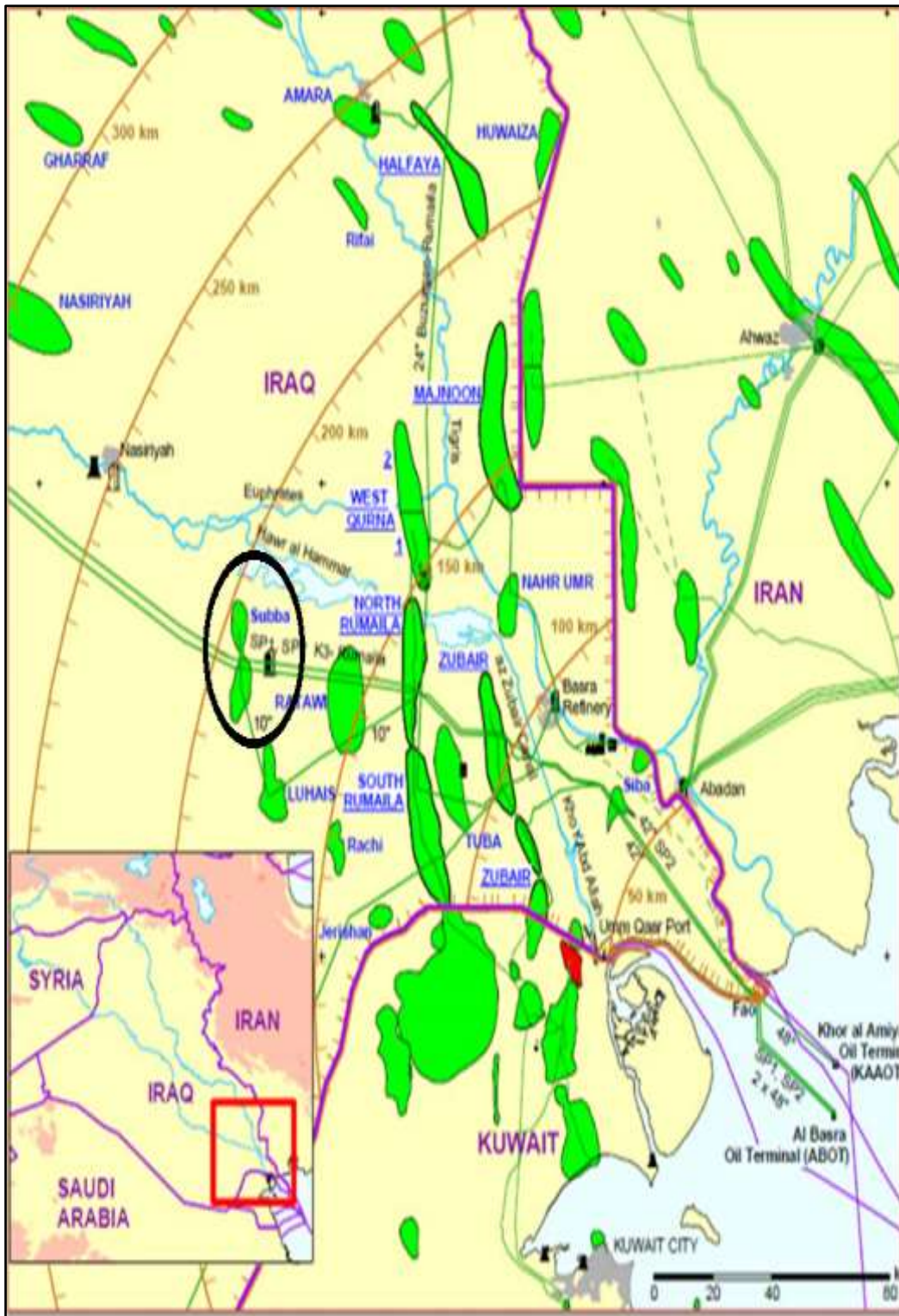


Figure 3 : Location map shows the Subba oilfield (INOC, 1979)

Age		Group	Formation	Lithology	Description	Average thickness (m)	
Period	Epoch						
Tertiary	L. Miocene - Recent	Kuwait	Dibdibba		Sand & pebble	200	
			Lower fars		Clay St, Lst arg	170	
			Ghar		Sand & subround pebble occ Clay	110	
	Early-M Miocene	Hasa	Dammam		Dolomite, porous vuggy	210	
			Rus		Anhydrite, white, massive Interbedded w\ Dolomite	165	
	Cretaceous	M-L Eocene	Hasa	Umm-Er-Radhuma		Dolomite grey saccharoidol, in part anhydritic	450
				Tayarat		Bituminous Shale at top, Dolomite, grey	220
		Late Cretaceous	Aruma	Shiranish		Limestone marly	120
				Hartha		Lst, gloc, Dol, porous, locally vuggy, Lst, grey, arg.	180
				Sadi		Limestone white, chalcky, fine, compact	260
Tanuma					Shale: black-brown fissile	50	
Khasib					Limestone: grey shaly	45	
Mishrif					Limestone: white detrital, porous, rudist	150	
Middle Cretaceous		Wasia	Rumalla		Limestone: , grey, marly	100	
			Ahmadi		Shale: Dark grey, fissile w/ Limestone: grey	140	
	Mauddud			Limestone grey	110		
	Nahr Umr			Shale black inter. w/ Sst	270		
Early Cretaceous	Thamama	Shuaiba		Lst , Dolomite fracture	85		
		Zubair		Shale, fissile, w/ sandstone fine-m. grained, Silt st, Clay st.	400		
		Ratawi		Limestone with streaks of Shale	200		
		Yamama		Limestone, light grey	120		
Jurassic	Upper Jurassic		Sulaiy		Limestone, argillaceous and marly	300	

Figure 4: Geological column for Subba oilfield

### 3. Input Data

The forms of data utilised to determine the strength and characteristics of elastic rocks, pore pressure, and in situ stresses include field reports, logs, and well-offset tests. Daily drilled reports, final drilling reports, daily geology reports, final geological reports, and master logs were all part of the field reports. Compressional Slowness (DTC, us/ft), Shear Slowness (DTS, us/ft), Density Log (ZDEN, (gm/cm<sup>3</sup>)), Bit Size (BS, in), Gamma Ray Log (GR, gAPI), Caliper Log (CAL, in). The offset tests comprised; core data (triaxial and Brazilian test), pore pressure tests evaluated using various techniques to calibrate the anticipated pore pressure profile, and Repeated Formation Tester (RFT). Fracture pressure calibration also uses the mini-frac data.

### 4. In-situ stress determination

The magnitudes of in-situ stresses, regardless of wellbore orientation, can majorly affect wellbore stability. It is essential to analyse the stress conditions along the entire relevant section of the wellbore to predict when the wellbore will fail accurately.

#### 4.1 Overburden Stress

The overburden pressure ( $\sigma_v$ ) generated by the weight of the overlying layers. The bulk density log is the source for calculating the overburden stress using Eq. (1). In most cases; the upper interval is not logged, therefore; linear extrapolation is used for calculating the overburden stress in the upper unlogged interval. Figure 5 shows the overpressure gradient for well SU\_20, which is close to being linear.

$$\sigma_v = \int_0^z \rho(z)g dz \quad (1)$$

Where  $\sigma_v$ = overburden stress, (Pa);  $\rho(z)$  is the bulk density log at depth  $z$ , (kg/m<sup>3</sup>);  $g$  = the constant of gravitational acceleration, 9.81 (m/s<sup>2</sup>);  $z$  = the depth at a depth of interest, m.

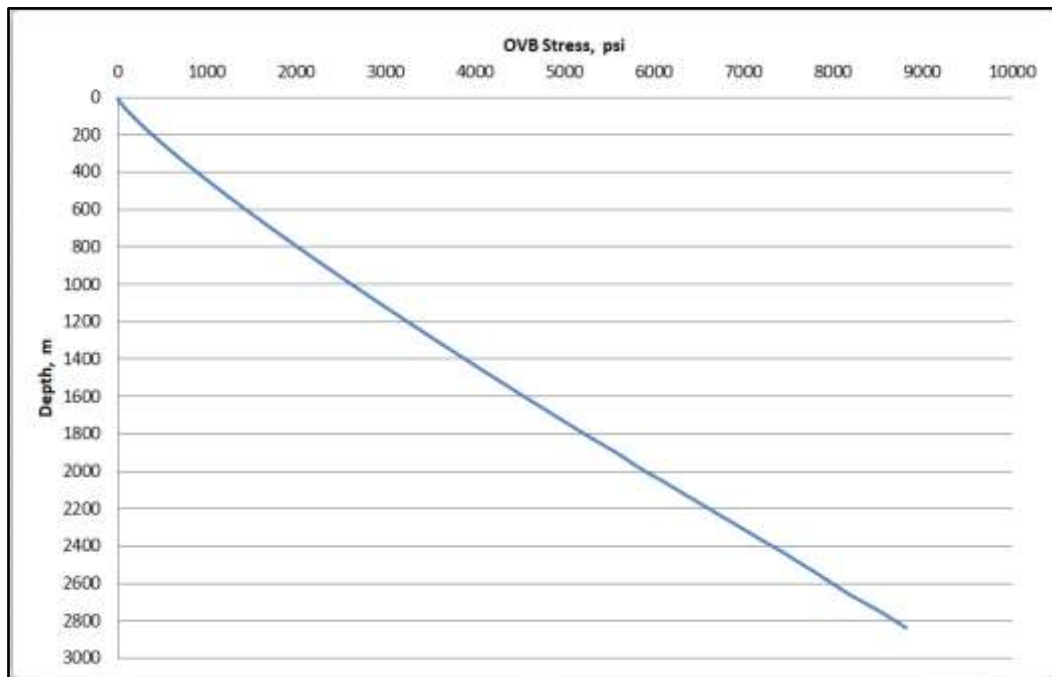


**Figure 5 :** Overburden stress for well SU\_20

#### 4.2 Pore Pressure Prediction

Analysis of pore pressure workflow performed by utilising well logging data (Resistivity and Acoustic logs) and calibrated with measured values obtained by a formation pressure test. A reasonable match is obtained from a modeled profile with the measured values for both wells. Eaton sonic model is used to model the pore pressure profile (Eq. 2). Figure 6 shows the pore pressure profile with the test points for well SU\_20.

$$P_p = \sigma_v - (\sigma_v - P_{hyd}) \left( \frac{\Delta_{tn}}{\Delta_{to}} \right)^x \quad (2)$$

Where  $P_p$ = pore pressure, psi;  $\sigma_v$ = overburden pressure, psi;  $P_{hyd}$ : hydrostatic pressure, psi;  $\Delta_{tn}$ = are the compressional slowness measured by the log, sec/ft;  $\Delta_{to}$  = values for compressional slowness based on the typical compaction trend, sec/ft;  $x$ = the adjustable exponent during calibration. Commonly  $x$  is 1.2 when using resistivity and 3.0 when using compressional slowness.

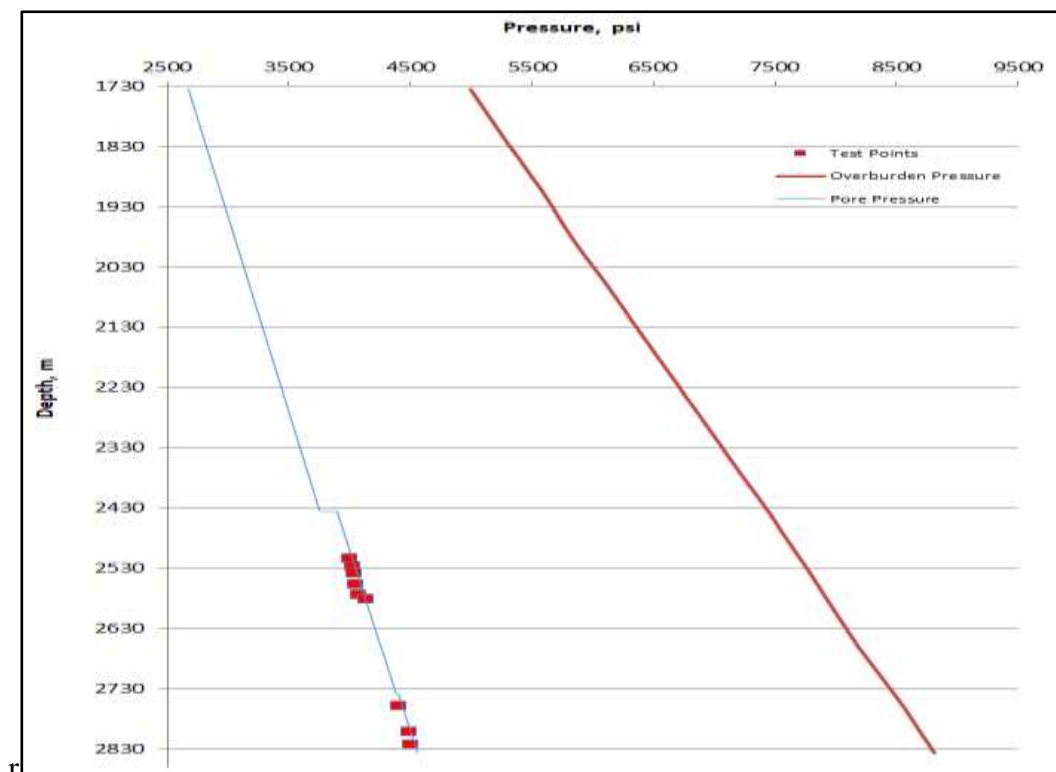


**Figure 6 :** Pressure Profile in Comparison for SU\_20

### 5. Rock Mechanical Properties

The main rock mechanical properties are elastic parameters and the strength of formations [9]. These properties are significant parameters in analysing wellbore stability and stress magnitude, and predicting the optimal mud weight window for risk-free drilling. Several empirical equations are applied to predict mechanical properties. These equations are based mainly on the wells logs: bulk density, compression wave velocities and shear wave velocity, gamma-ray, and porosity.

#### 5.1 Elastic Rock Properties

The Acoustic wireline logs are used to calculate dynamic Poisson's ratio and dynamic Young's modulus. For starters, it is important to calculate approximations for the Bulk modulus

(K) and Shear modulus (G). These values can be calculated using the empirical relationships described below [10]:

$$G_{dyn} = 13474.45 \frac{\rho_b}{(\Delta t_s)^2} \quad (3)$$

$$K_{dyn} = 13474.45 \frac{\rho_b}{(\Delta t_c)^2} - \frac{4}{3} G_{dyn} \quad (4)$$

Dynamic characteristics can be determined using empirical relationships with the Bulk modulus (K) and Shear modulus (G), as illustrated below [11]:

$$E_{dyn} = \frac{9G_{dyn}K_{dyn}}{G_{dyn}+3K_{dyn}} \quad (5)$$

$$\nu_{dyn} = \frac{3K_{dyn}-2G_{dyn}}{6K_{dyn}+2G_{dyn}} \quad (6)$$

Where  $\rho_b$ = bulk density, g/cm<sup>3</sup>;  $\Delta t_s$ = shear slowness,  $\mu$ s/ft;  $\Delta t_c$ = compressional slowness,  $\mu$ s/ft;  $G_{dyn}$ = dynamic Shear Modulus, Mpsi;  $K_{dyn}$ = dynamic Bulk Modulus, Mpsi;  $E_{dyn}$ = dynamic Young's Modulus, Mpsi;  $\nu_{dyn}$ =dynamic Poisson's Ratio; 13474.45= conversion factor.

The static properties is generally less than a dynamic form because of pore pressure, cementation, rate of stress-strain, and amplitude [12]. Static properties can be estimated from dynamic properties [13], [12] as follows.

$$E_{static} = 0.032 \times E_{dyn}^{1.632} \quad (7)$$

$$\nu_{sta} = \nu_{dyn} * \nu_{multiplier} \quad (8)$$

Where  $E_{sta}$  = Static Young's modulus, Mpsi;  $\nu_{sta}$  = Static Poisson's ratio, unitless. The Static Young's modulus profile for well SU\_20 is presented below in Figure 7.

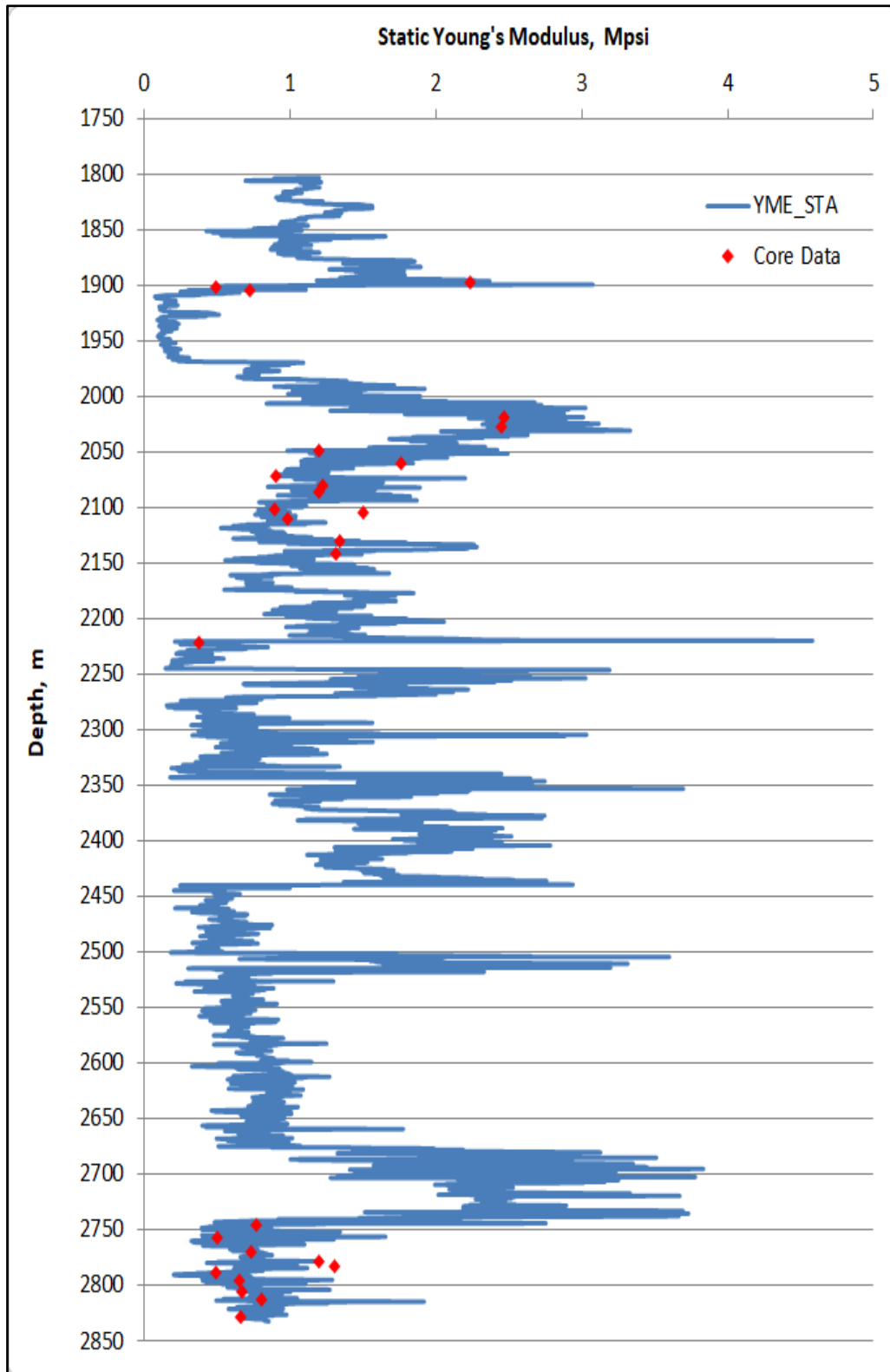


**Figure 7:** Static Young's modulus over whole depth for well SU\_20

### 5.2. Rock Strength

The Rock Strength is unconfined compressive strength (UCS), cohesion ( $C_0$ ), tensile strength ( $T_0$ ), and friction angle ( $\varphi$ ). Well-logging data was used to find suitable correlations to calculate all section formations' strength parameters as follows:

$$\varphi = 700.417GR \tag{9}$$

$$UCS = 4.242 * E_{sta} \tag{10}$$

$$C_o = \frac{UCS}{2[\sqrt{1+(\tan\varphi)^2} + \tan\varphi]} \tag{11}$$

$$T_o = K * UCS \tag{12}$$

Where  $\varphi$  = Internal friction angle, deg;  $UCS$  = Unconfined compressive strength, psi;  $C_o$  = Cohesion, psi;  $T_o$  = Tensile strength, psi;  $GR$  = Gamma-ray, gAPI.

Figure 8 illustrates the Rock Strength properties with the calibrated points, where friction angle in the first track from the left, the cohesion in the second track, the unconfined compressive strength in the third track and tensile strength in the fourth track.

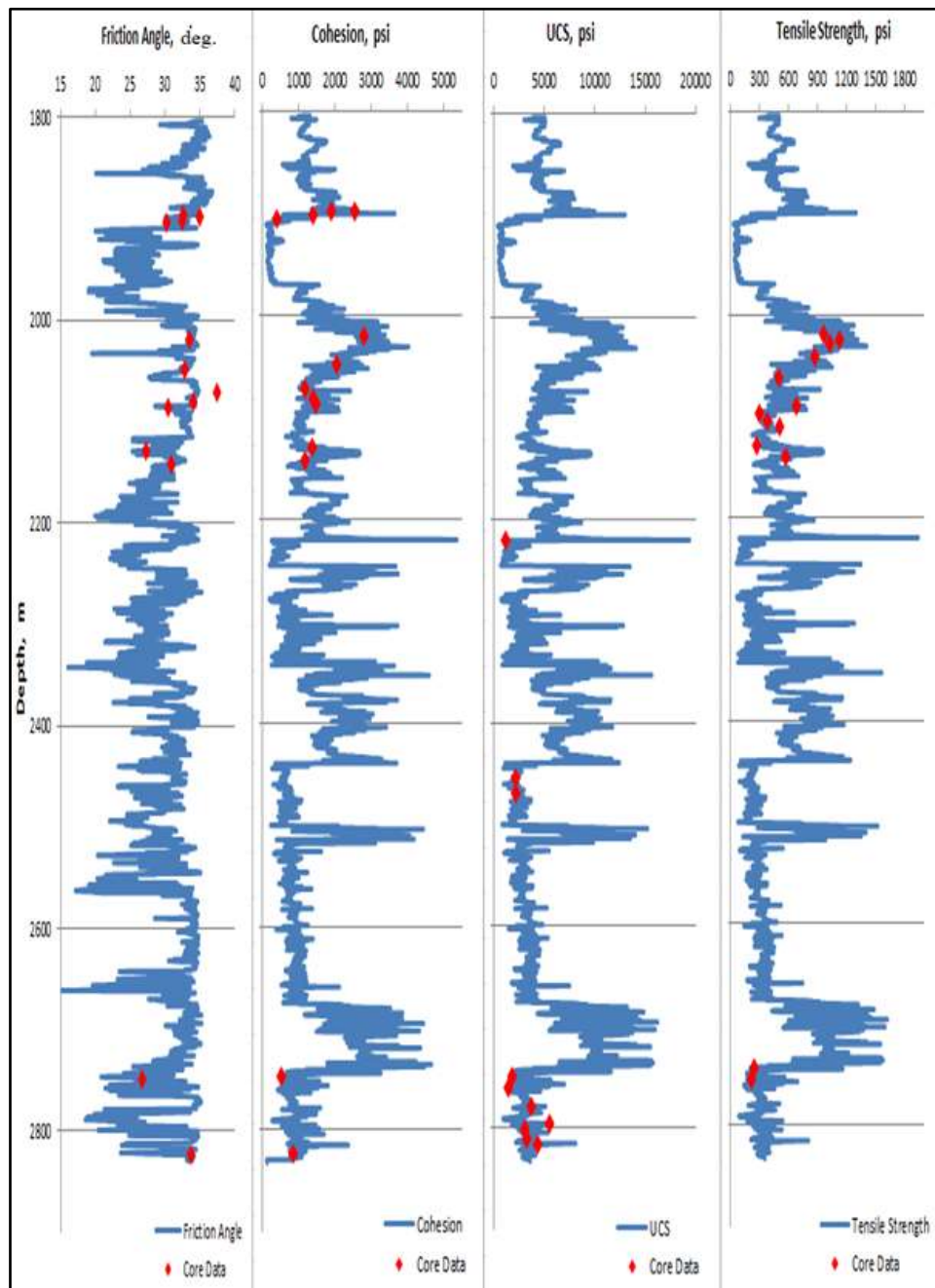


**Figure 8 :** Rock strength parameters over whole depth for well SU\_20

## 6. Horizontal Stresses

The stability of a wellbore can be significantly influenced, irrespective of the direction in which the wellbore is drilled, by the quantity of in-situ forces and the direction in those stresses are act in. To accurately anticipate when the wellbore failure will occur, it is necessary to model the stress conditions along the intended length of the well.

### 6.1 The Principal Horizontal Stresses' Orientations

Wellbore failure can be influenced by the direction in which the principal horizontal stresses are applied [14]. Assuming the well is vertical, the direction of the breakouts and tensile cracks in the wellbore clearly indicates the horizontal stress azimuths. For breakouts to occur, it is necessary for the hoop stress to be more compressive in the direction of the minimum horizontal stress and for the stress concentration to be significant enough to exceed the rock strength [14]. In contrast, the orientation of the largest horizontal principal stress is related to the lowest compression of the circumferential stress, resulting in drilling-induced fractures.

### 6.2 Minimum and maximum horizontal stress magnitudes

Minimum horizontal stress magnitudes are key characteristics for determining a stress regime. This minimal horizontal stress matches up to the fracture closure pressure measured in the Extended Leak-off Tests (XLOT) [15]. The magnitude of the highest and minimum horizontal stresses can be determined from Eq. (12,13) respectively and as presented below in Figure 9.

$$\sigma_h = \frac{\nu}{1-\nu} \sigma_v - \frac{\nu}{1-\nu} \alpha P_p + \alpha P_p + \frac{E}{1-\nu^2} \varepsilon_h + \frac{\nu E}{1-\nu^2} \varepsilon_H \quad (13)$$

$$\sigma_H = \frac{\nu}{1-\nu} \sigma_v - \frac{\nu}{1-\nu} \alpha P_p + \alpha P_p + \frac{E}{1-\nu^2} \varepsilon_H + \frac{\nu E}{1-\nu^2} \varepsilon_h \quad (14)$$

Where  $\sigma_H$ = Maximum Horizontal Stress, psi;  $\varepsilon_h$ - Tectonic strain factors in minimum horizontal direction;  $\sigma_h$ = Minimum Horizontal Stress, psi;  $\alpha$ = Biot's coefficient ( $\alpha = 1$ , conventionally);  $\varepsilon_H$ = Tectonic strain factors in maximum horizontal direction.

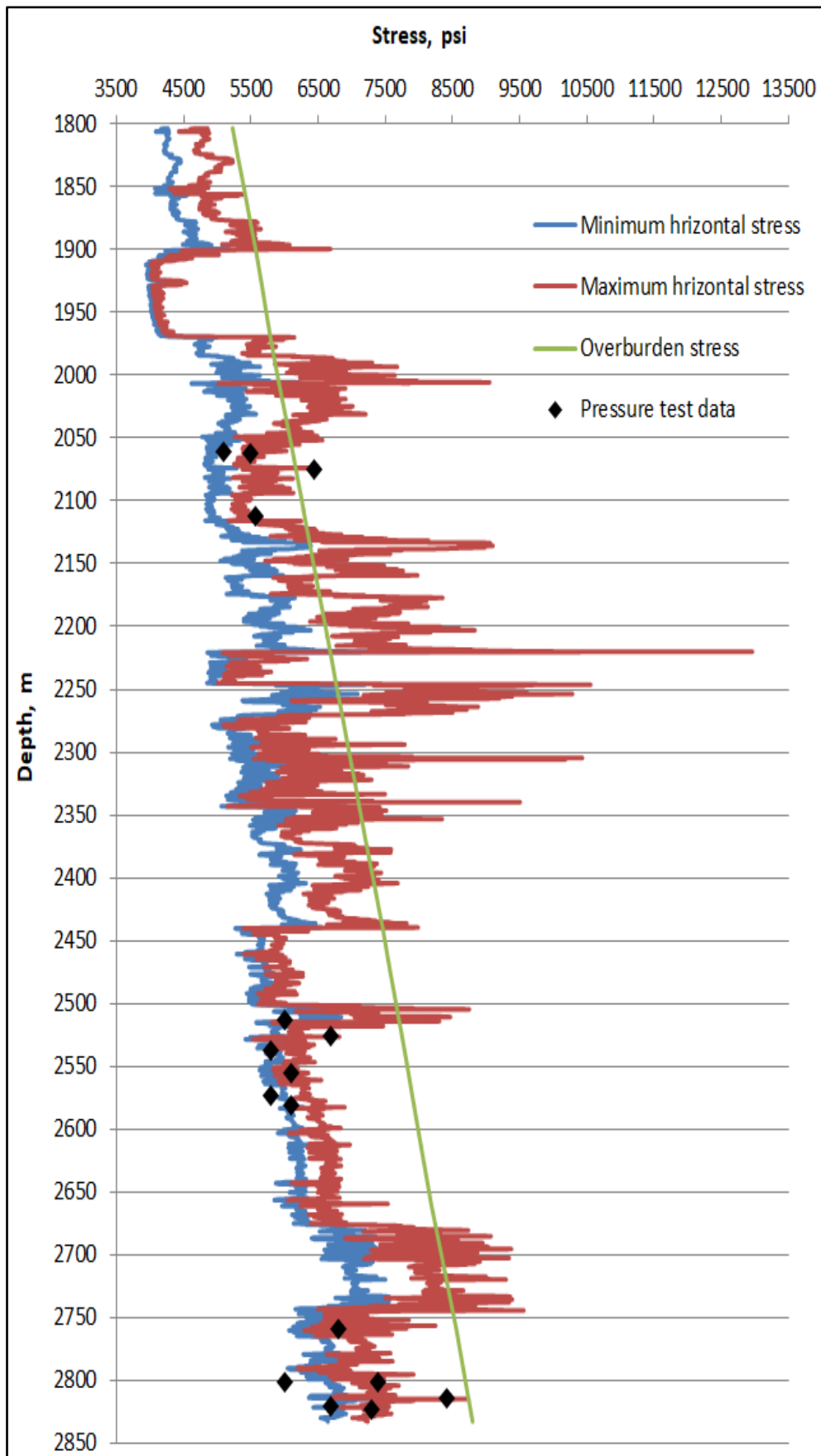


Figure 9 : Overburden stress in addition to principal horizontal stresses and pressure test data for well SU\_20

## 7. Failure Criteria

Rock failure occurs when the formations' strengths are lower than the forces in the area around the wellbore. Rock failure criteria develop a suitable mud window for wellbore stability. Failure criteria vary by rock type and lithology [16]. The tension surrounding the wellbore can be modelled using these criteria. The suitable failure criteria in an analysis should be determined by matching actual failure to predicted failure.

### 7.1 Stress Transformation in Boreholes

Drilling fluid should be dense enough to maintain the mechanical stability of the borehole wall, as the excavation of the subsurface formation causes rearrangement of the stress state. The density of the drilling fluid used to maintain borehole stability depends on the known in-situ principal stresses. For this reason, determining the stress around the borehole is crucial in examining the wellbore's stability.

1-The three principal stresses at the borehole wall in state of tensile failure (represented by hydraulic fracturing), [17], [18] are given by;

$$\sigma_r = P_w \quad (15)$$

$$\sigma_\theta = D - P_w \quad (16)$$

$$\sigma_z = E \quad (17)$$

Where

$$D = 3\sigma_h - \sigma_H \quad (18)$$

$$E = \sigma_v - 2\nu(\sigma_H - \sigma_h) \quad (19)$$

2-The three principal stresses at the borehole wall in state of shear failure (in the form of collapse or breakout formation), [17], [18] are given by;

$$\sigma_r = P_w \quad (20)$$

$$\sigma_\theta = A - P_w \quad (21)$$

$$\sigma_z = B \quad (22)$$

Where

$$A = 3\sigma_H - \sigma_h \quad (23)$$

$$B = \sigma_v + 2\nu(\sigma_H - \sigma_h) \quad (24)$$

$P_w$ = internal wellbore pressure, psi;  $\sigma_r$ = radial stress, psi;  $\sigma_\theta$ = tangential stress, psi;  $\sigma_z$ = axial stress, psi.

Figure 10 explain the Principal Induced stresses for the whole depth for well SU\_20.

### 7.2 Shear and Tensile Failure

If  $P_{wbo} \geq P_w$ ; shear failure occurs, on the other hand, if the internal well pressure exceeds fracture pressure (i.e.,  $P_w \geq P_{frac}$ ) the borehole fracturing will occur. There are several criteria for calculating minimum & maximum mud weight. Modified Lade criterion [19] is applied as:

$$\frac{I'_1{}^3}{I'_3} = 27 + \eta \quad (25)$$

$$I'_1 = (\sigma_1 + S) + (\sigma_2 + S) + (\sigma_3 + S) \quad (26)$$

$$I'_3 = (\sigma_1 + S)(\sigma_2 + S)(\sigma_3 + S) \quad (27)$$

Both (S) and ( $\eta$ ) are constants of the material, with (S) representing the rock's cohesiveness and ( $\eta$ ) its internal friction. The following formulas can be used to directly determine these parameters from the Mohr-coulomb cohesion and internal friction angle:

$$S = \frac{c}{\tan \varphi} \quad (28)$$

$$\eta = \frac{4 \tan \varphi^2 (9 - 7 \sin \varphi)}{1 - \sin \varphi} \tag{29}$$

The following is an alternative formulation for this criterion to consider:

$$FI = 27 + \eta - \frac{l'_1{}^3}{l'_3} \tag{30}$$

This criterion states that shear failure happens if  $FI \leq 0$ .

The key advantage of utilising the Modified Lade criteria is that it considers the effect of middle principal stress on the tensile strength of the rock.

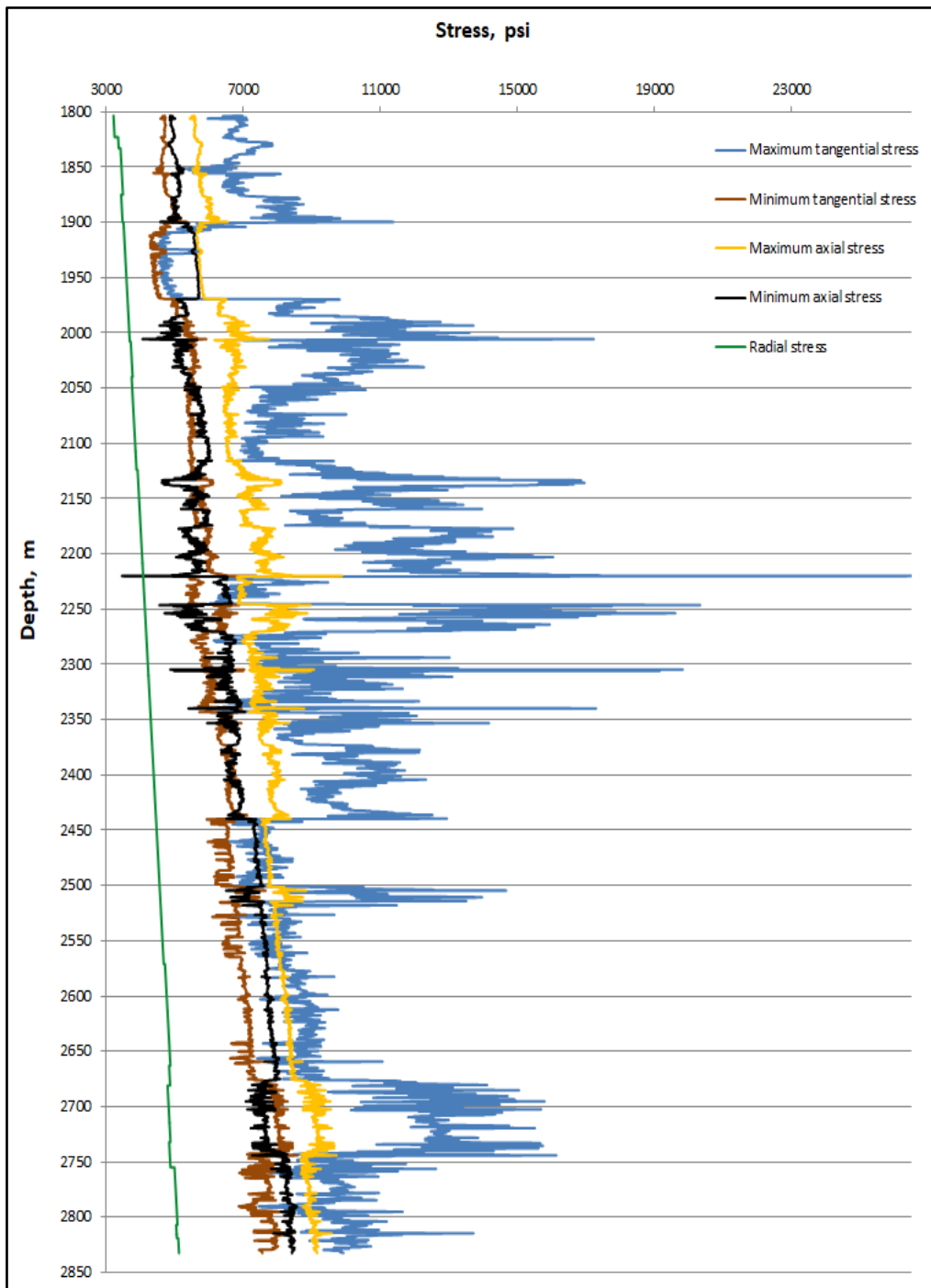


**Figure 10 :** Principal Induced effective stresses for the whole depth for well SU\_20  
**8. Geomechanical Model Results**

*8.1 Mud Window*

Instability in the borehole during drilling can cause significant issues in any part of the world. By studying geomechanics, a window of acceptable mud weight can be determined [20]. The mud weight window (MWW) is one of the outputs of wellbore stability analysis [21, 22], which consists of minimum (collapse EMW) and maximum (fracture EMW) mud weight, as shown below in Figure 11 for well SU\_20.

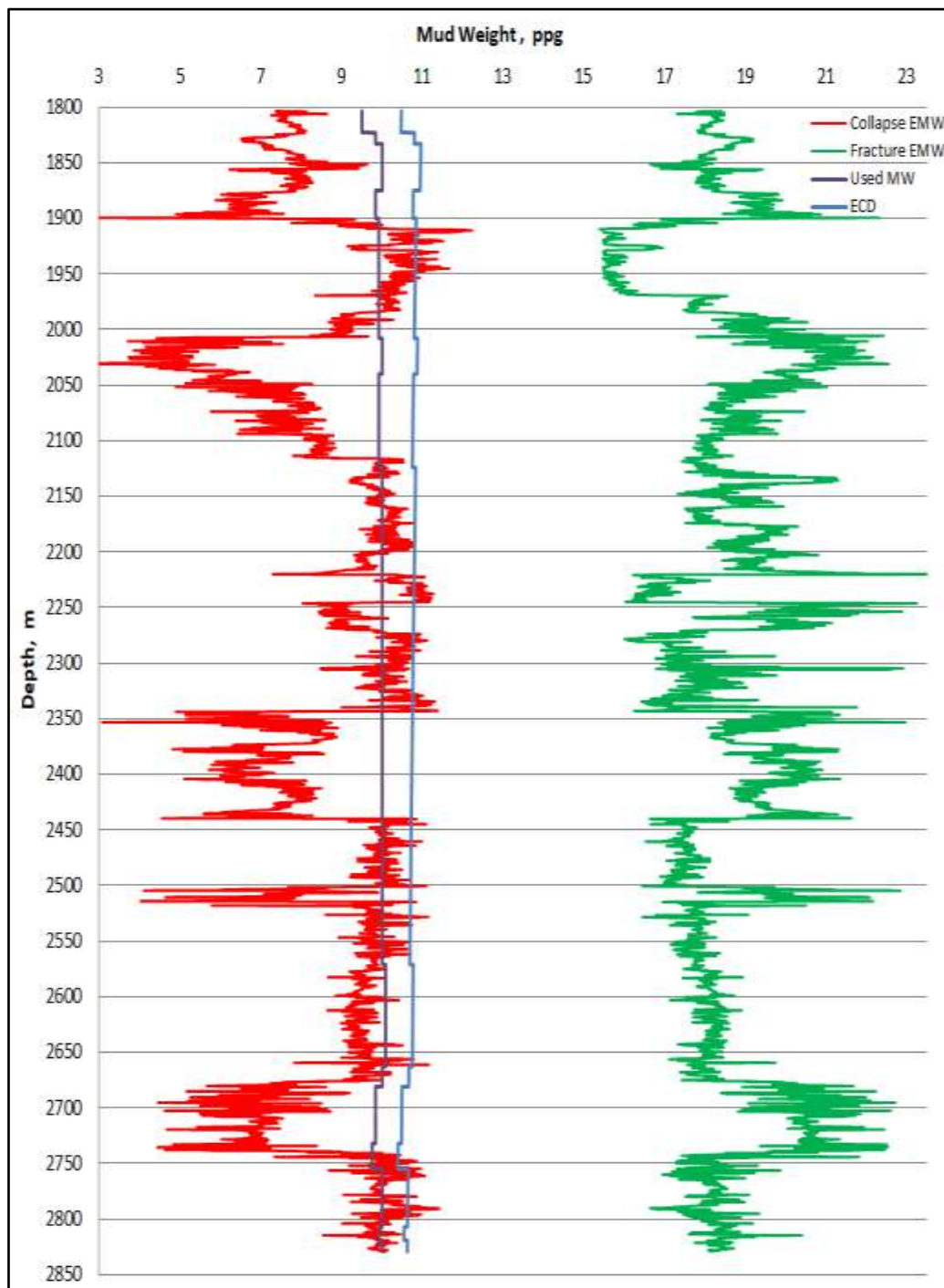


**Figure -11** Mud weight for whole depth for well SU\_20

8.2 Breakout interval

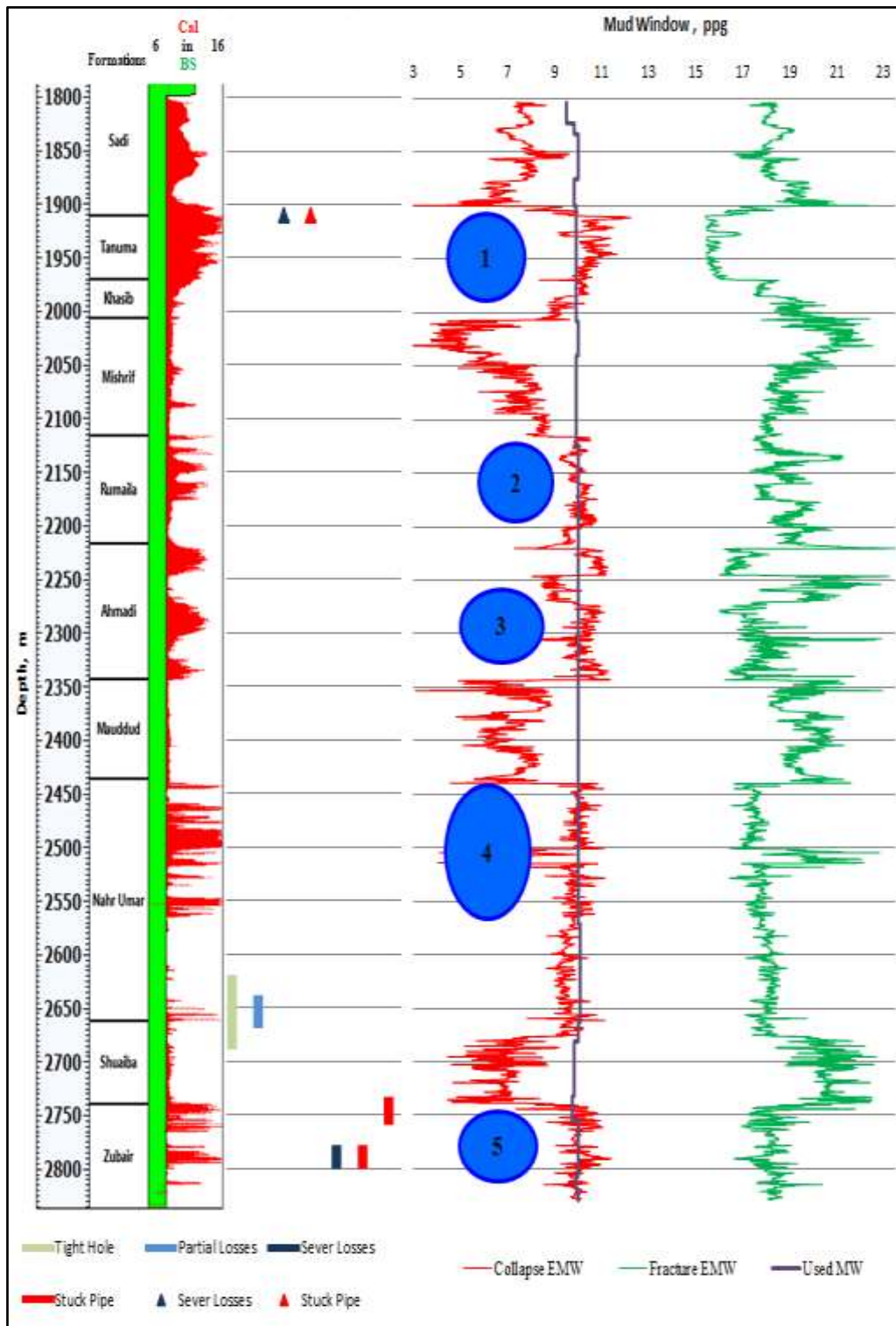


Figure 12 : Stability plot with numbered main instability zones for SU\_20

To evaluate the model's accuracy, expected unstable zones are contrasted with data from drilling events, data sets, and the calliper log about instability incidents. Five primary regions of possible instability emerge from the stability plots presented in the previous section. As seen in the following Figure (Figure 12), they were marked.

### 8.3 Stress perturbations

When we took a brief look at the reservoir part's stress environment, we noticed that there is some stress disturbance; therefore, we can partition the stresses in this area according to Table 1.

**Table 1:** Fault regime type

Zones Name	Fault regime
Sadi	Normal fault / Strike-slip
Tanuma	Normal fault
Khasib	Strike-slip
Mishrif	Normal fault / Strike-slip
Rumaila	Strike-slip / Normal fault
Ahmadi	Strike-slip
Mauddud	Normal fault
Nahr Umar	Normal fault
Shuaiba	Strike-slip
Zubair	Normal fault

Figure 13 and Figure 14; show the output of the 1D mechanical earth modelling for well SU\_21 and well SU\_22, respectively.

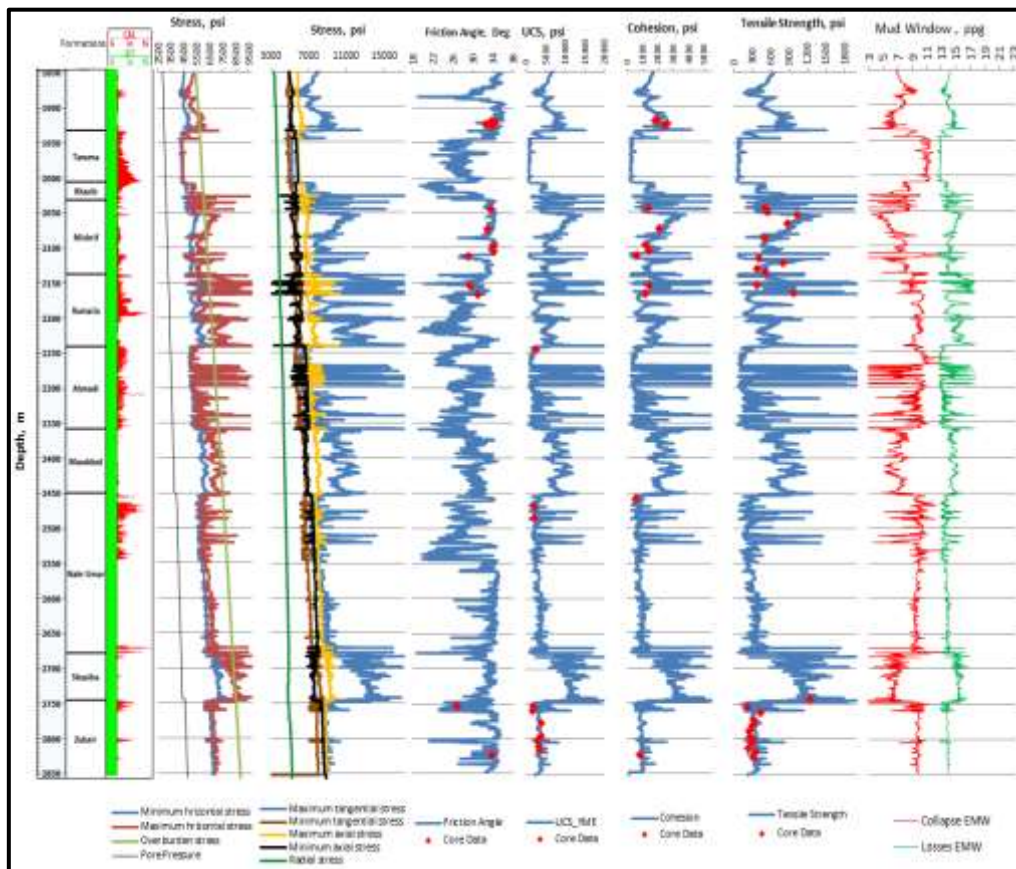


**Figure 13 :** MEM for well SU-21

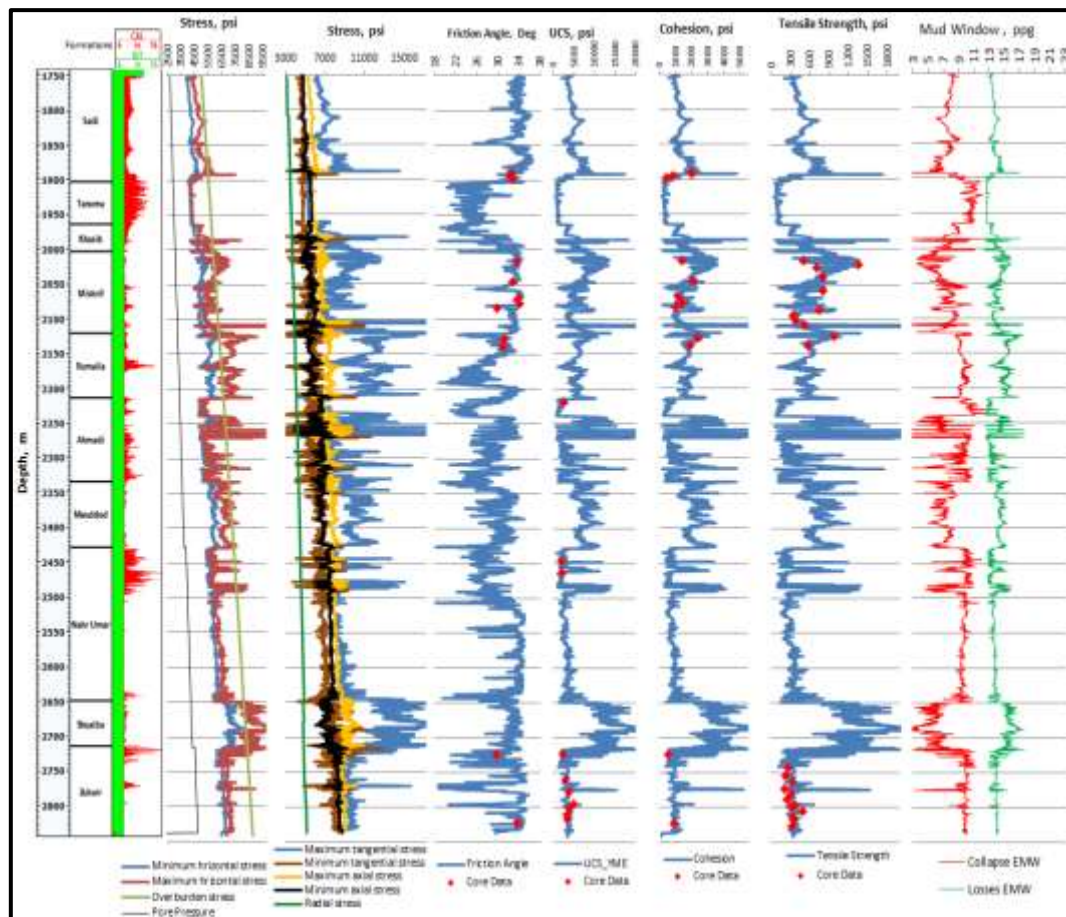


Figure 14 : MEM for well SU-22

## 9. Discussion

The wellbore instability analysis for real failure observed from the calliper log and predicted failure using the Modified Lade criterion revealed that only shear failure had been experienced using current and proposed mud weight. The five main zones of potential instability can be recognised in the Subba oilfield are:

*Trouble Zone 1:* Most of the time, the weight of the mud used was minimal. This suggests that borehole breakouts will happen, particularly if the pump stops working. The calliper log would show an enlarged borehole if this were the case. The well's final report details any problems or complications during the drilling process. Drilling activities were reportedly impeded because of material falling into the wellbore along this segment (Tanuma formation and upper part of Khasib formation) due to breakouts. According to the calculations, higher mud weight is recommended.

*Trouble Zone 2:* Increasing mud weight was the best solution for safe drilling without wellbore failure, which occurs in several depth of this zone (Rumaila formation) due to the presence of argillaceous limestone.

*Trouble Zone 3:* Ahmadi Formation, the upper part of which is a shale and then followed by limestone, and here we will face the problem of breakout in front of the shale layers at the top of the formation, as well as in layers that contain argillaceous limestone, so increasing the weight of the drilling mud will be an appropriate option to solve the problems of this formation under the availability of a good mud window.

*Trouble Zone 4:* In zone 4 (Nahr Umar formation), the applied mud weight is less than the collapse EMW many times in that section. Both the report and the calliper data confirm the breakouts. Partial losses were recorded, and many drilling breaks were required. The model predicts the collapse of EMW very close to calliper data. The results show that, in general, the mud weight chosen was low and very near to collapse EMW; hence, breakouts were common.

*Trouble Zone 5:* Shale and sandstone are both components of the Zubair Formation. Shale occupies the upper and lower part of the formation and permeates the sandstone layers. Returning to the drilling reports and caliper data, there was a breakout of the wellbore, stuck pipes, and severe losses of drilling mud during the drilling of this section. The model gave consistent results with calliper data, where the density used was less than the collapse EMW on several parts in this section.

## 10. Conclusion

1- The wellbore instability analysis for real failure observed from the calliper log and predicted failure using the Modified Lade criterion revealed that only shear failure had been experienced using current and proposed mud weight.

2- Risk assessment for Tanuma formation parameters reveals that the chance of stability by 50% can be achieved by increasing mud weight.

3- Increasing the current mud weight will significantly prevent possible breakout failure.

4- During the drilling process, the model should be updated to enhance it. It relies on specific log measurements and core data for calibration, so its quality depends on the availability and quality of the input data. The potential savings are high if the data can be managed and used efficiently.

5- To conclude, the relatively simple 1D MEM built in this research enabled predictions that could be validated even though some data (core and LOT data) for calibration was only available for some sections. It did not require large amounts of data and professional software to build, so using the means available to the industry. It is possible to use available data to quickly and economically create a 1D MEM for a well and use it as part of the well planning process to reduce instability and the associated costs.

## 11. Recommendations AND FUTURE WORK

The wellbore stability model developed in this study can be potentially applied to other wells by using a similar strategy that may be modified to the new wells' specifications and other field circumstances, utilising a similar methodology that could be modified to the specific field conditions. Construct a robust three dimension geomechanical model (3D MEM) based on these study elements, which will introduce a great integration between the structural geological model and the mechanical earth model to provide better and more extensive wellbore stability assessment.

## 12. Acknowledgements

This paper would not have been possible without all the support and encouraging words from my supervisor Prof. Dr. Mohammed Saleh Jawad Al-Jawad, and the Thi-Qar Oil Company.

### 13. Nomenclature and Abbreviations

Nomenclature		
Symbol	Description	unit
$E_{dyn}$	Dynamic Young's modulus	Mpsi
$G_{dyn}$	Dynamic shear modulus	Mpsi
$K_{dyn}$	Dynamic bulk modulus	Mpsi
$\nu_{dyn}$	Dynamic Poisson's ratio	Unitless
$\nu_{sta}$	Static Poisson's ratio	Unitless
$\varphi$	Friction angle	degree
$T_o$	Tensile strength	Psi
$C_o$	Cohesive strength	Psi
UCS	Unconfined compressive strength	Psi
$\sigma_v$	Overburden stress	Psi
$\sigma_H$	Maximum principal horizontal stress	Psi
$\sigma_h$	Minimum principal horizontal stress	Psi
$\varepsilon_h$	Tectonic strain factors in minimum horizontal direction	Unitless
$\varepsilon_H$	Tectonic strain factors in maximum horizontal direction	Unitless
$\sigma_\theta$	Wellbore Induced tangential stress	Psi
$\sigma_r$	Wellbore Induced radial stress	Psi
$\sigma_z$	Wellbore Induced axial stress	Psi
$\sigma_1$	Maximum principal stress	Psi
$\sigma_2$	Intermediate principal stress	Psi
$\sigma_3$	Minimum principal stress	Psi
$P_p$	Pore pressure	Psi
$P_{hyd}$	Hydrostatic pressure	Psi
$P_w$	Internal wellbore pressure	Psi
$P_{wbo}$	Breakout pressure	Psi
$P_{frac}$	Fracture pressure	Psi
$\rho_b$	Bulk density	g/cm <sup>3</sup>
$\Delta t_s$	Shear slowness	μs/ft
$\Delta t_c$	Compressional slowness	μs/ft
$\Delta t_{tn}$	compressional slowness measured by the log	μs/ft
$\Delta t_o$	compressional slowness based on the typical compaction trend	μs/ft
$\alpha$	Biot coefficient	Unitless

Abbreviations	
Acronym	Definition
1D MEM	One dimension mechanical earth model
3D MEM	Three dimension mechanical earth model
INOC	Iraqi National Oil Company
BS	Bit size
CAL	Caliper log
GR	Gamma ray log
ZDEN	Density log

<b>DTC</b>	Compression sonic log
<b>DTS</b>	Shear sonic log
<b>EMW</b>	Equivalent mud weight
<b>MWW</b>	Mud weight window
<b>LOT</b>	Leak off test
<b>XLOT</b>	Extended leak off test
<b>RFT</b>	Repeated formation test
<b>NPT</b>	Nonproductive time
<b>FI</b>	Failure index
<b>g</b>	gravitational acceleration
<b>x</b>	adjustable exponent during calibration
<b>13474.45</b>	conversion factor

## References

- [1] R. H. Allawi and M. S. Al-Jawad, "Wellbore instability management using geomechanical modeling and wellbore stability analysis for Zubair shale formation in Southern Iraq," *Journal of Petroleum Exploration and Production Technology*, vol. 11, pp. 4047-4062, 2021.
- [2] S. D. Shaban and H. A. Hadi, "Geomechanical Analysis to Avoid Serious Drilling Hazards in Zubair Oilfield, Southern Iraq," *Iraqi Journal of Science*, pp. 1994-2003, 2020.
- [3] A. Al-Ajmi, "Wellbore stability analysis based on a new true-triaxial failure criterion," KTH, 2006.
- [4] M. A. Menshed and H. D. Al-Mozan, "Geological Modeling for Nahr Umr Formation in Subba Oil Field, Southern Iraq," *The Iraqi Geological Journal*, pp. 66-86, 2021.
- [5] O. N. Al-Khazraji, S. A. Al-Qaraghuli, L. Abdulkareem, and R. M. Idan, "Uncertainty Analysis to Assess Depth Conversion Accuracy: A Case Study of Subba Oilfield, Southern Iraq," *Iraqi Journal of Science*, pp. 618-631, 2022.
- [6] H. A. Chafeet, N. A. Dahham, and A. M. Handhal, "Palynofacies and Source Rocks Evaluation for Selected Samples of Subba Oil Field, Southern Iraq," *Iraqi Journal of Science*, pp. 1063-1079, 2020.
- [7] R. M. Idan, F. A. Al-Musawi, A. L. Salih, and S. A. Al-Qaraghuli, "The petroleum system of Zubair Formation in Zubair subzone, southern Iraq," *Journal of Petroleum Research and Studies*, vol. 9, no. 4, pp. 57-73, 2019.
- [8] R. M. Idan and R. F. Faisal, "Application of Geophysical Logs to Estimate the Source Rock Quantity of Ratawi Formation, Southern Iraq: A Comparison Study," in *IOP Conference Series: Materials Science and Engineering*, 2019, vol. 579, no. 1: IOP Publishing, p. 012025.
- [9] A. K. Mohammed and N. S. Selman, "Building 1D mechanical earth model for Zubair oilfield in Iraq," *J Eng*, vol. 26, no. 5, 2020.
- [10] E. Fjaer, R. M. Holt, P. Horsrud, and A. M. Raaen, *Petroleum related rock mechanics*. Elsevier, 2008.
- [11] M. D. Zoback, *Reservoir geomechanics*. Cambridge university press, 2010.
- [12] A. R. Najibi, M. Ghafoori, G. R. Lashkaripour, and M. R. Asef, "Reservoir geomechanical modeling: In-situ stress, pore pressure, and mud design," *Journal of Petroleum Science and Engineering*, vol. 151, pp. 31-39, 2017.
- [13] J. P. Castagna, M. L. Batzle, and R. L. Eastwood, "Relationships between compressional-wave and shear-wave velocities in elastic silicate rocks," *geophysics*, vol. 50, no. 4, pp. 571-581, 1985.
- [14] C. A. Barton, D. Moos, P. Peska, and M. D. Zoback, "Utilising wellbore image data to determine the complete stress tensor: application to permeability anisotropy and wellbore stability," *The log analyst*, vol. 38, no. 06, 1997.
- [15] E. Van Oort and R. Vargo, "Improving formation-strength tests and their interpretation," *SPE Drilling & Completion*, vol. 23, no. 03, pp. 284-294, 2008.
- [16] R. H. Allawi and M. S. Al-Jawad, "4D Finite element modeling of stress distribution in depleted reservoir of south Iraq oilfield," *Journal of Petroleum Exploration and Production Technology*, pp. 1-22, 2021.

- [17] W. Bradley, "Mathematical concept-Stress Cloud-can predict borehole failure," *Oil Gas J.;*(United States), vol. 77, no. 8, 1979.
- [18] B. Aadnoy and M. Chenevert, "Stability of highly inclined boreholes," *SPE Drilling Engineering*, vol. 2, no. 04, pp. 364-374, 1987.
- [19] R. T. Ewy, "Wellbore-stability predictions by use of a modified Lade criterion," *SPE Drilling & Completion*, vol. 14, no. 02, pp. 85-91, 1999.
- [20] A. K. Abbas, S. D. Alhussainy, H. A. Abdul Hussien, and R. E. Flori, "Safe mud weight window determination: a case study from southern Iraq," in *53rd US rock mechanics/geomechanics symposium*, 2019: OnePetro.
- [21] V. Rasouli, Z. J. Pallikathekathil, and E. Mawuli, "The influence of perturbed stresses near faults on drilling strategy: a case study in Blacktip field, North Australia," *Journal of Petroleum Science and Engineering*, vol. 76, no. 1-2, pp. 37-50, 2011.
- [22] J. Zhang, "Borehole stability analysis accounting for anisotropies in drilling to weak bedding planes," *International journal of rock mechanics and mining sciences*, vol. 60, pp. 160-170, 2013.